Effects of Silane Coupling Agents on Mica-Filled Styrene-Butadiene Rubber

SHANKAR DEBNATH, SADHAN K. DE, and DIPAK
KHASTGIR, *Rubber Technology Centre, Indian Institute of
Technology, Kharagpur 721302, India*

Synopsis

The effects of silane coupling agents on styrene-butadiene rubber (SBR)-mica composites have been studied with special reference to the technical properties and polymer–filler interaction. Silane-treated mica improves polymer–filler interaction, which subsequently enhances the tensile and other technically important mechanical properties. Failure surfaces of tensile, tear, and wear specimens have been examined under scanning electron microscope (SEM) and the fractographs have been correlated with the strength and failure mode of the composites.

INTRODUCTION

Recently mica has shown promise as a useful filler for thermoplastics due to its low cost, availability, and outstanding electrical, heat, and chemical resistance.[1] Extent of reinforcement by mica depends on the aspect ratio[2] (ratio of length to thickness). Breakdown of mica particles during mixing and processing reduces the aspect ratio.[3] Use of hot runners, longer sprues, and streamlining may reduce the particle breakdown.[4] Enhancement of mica–polymer interaction by treatment of chlorinated paraffin,[5] maleated polypropylene,[6] silane,[7-8] and titanate[9] coupling agents has been studied in detail. Ultrasonically delaminated mica[10] has been found to impart superior properties to polypropylene composites over conventionally prepared mica. VuKhanh et al.[11-13] have made an in-depth study on the fracture behavior of mica-polypropylene composites. Xavier and Sharma[14] have shown the structure–property relationship of mica–polypropylene composites.

Flow properties[15-17] of mica-filled polyolefins have been extensively investigated. Utracki[18] has pointed out the anisometric flow of PP-mica composites. Flow, mechanical, and electrical properties of plasma-treated mica-polyolefins composites[15, 19, 20] have been found to be better than conventional mica-polyolefins composites.

However, reports on the use of mica as filler in rubber are scant. It has been reported that mica enhances anisometric swelling of nitrile rubber vulcanizates[21] and reduces permeability[22] of gases and liquids.

In earlier communications we have reported the network structure-technical property relationship,[23] kinetics of vulcanization,[24] electrical properties,[25] and anisotropic[26] behavior of mica-filled styrene-butadiene rubber.

In the present work we have chosen one sulfur-bearing and one nonsulfur coupling agent in order to study their effects on vulcanization, polymer-filler

interaction, and structure-property relationship. Scanning electron photomicrographs have been used to follow the failure mechanism.

EXPERIMENTAL

Preparation of Mixes, Rheometry, and Preparation of Test Samples

Formulations of the mixes are given in Table I. Mixing was done on an open two-roll mill with a nip gap of 0.25 mm and at a friction ratio of 1 : 1.10 at 70°C.

Optimum cure time at 150°C was obtained from rheographs (Fig. 1) using Monsanto Rheometer R-100. Vulcanization of mixes was done in an electrically heated press at 150°C and at a pressure of 4.5 MPa. Vulcanizates were cooled rapidly in water at the end of curing cycles and then conditioned for 24 h before testing. All properties were measured along the grain direction.

Physical Testing of the Samples

Stress–strain data were determined on Instron Universal Testing machine (model 1195) using an ASTM C-type dumbbell specimen according to ASTM D412-81. Tear strength was determined according to ASTM D624-81 test method using 90° angle test piece. Abrasion resistance was determined in a DuPont Cryodon abrader according to ASTM D-394, method A.

A Dunlop tripsometer was used to measure rebound resilience at 35°C according to B.S. 903, Pt. 22, 1950. A Goodrich flexometer was used to measure heat build-up and dynamic set according to ASTM D623-67, method A.

Compression set at constant stress (187 kg) and the same at constant strain (25%) were measured according to ASTM methods D395-61, method A and D395-61, method B, respectively.

Chemical Testing of the Samples

Volume fraction of swollen rubber (V_r) in the vulcanizates was determined by equilibrium swelling method in benzene at 37°C using the following equation,[27]

$$V_r = \frac{(D - FT)\rho_r^{-1}}{(D - FT)\rho_r^{-1} + A_o\rho_s^{-1}} \tag{1}$$

where,

T = weight of the test specimen,
F = weight fraction of insoluble components in the samples,
D = deswollen weight of the test specimen,
A_o = weight of absorbed solvent, corrected for swelling increment,
ρ_r = density of rubber, and
ρ_s = density of solvent.

TABLE I
Formulations of the Mixes

	Gum	Untreated mica				A-187-treated mica				Si-69-treated mica			
Mix no.	A	B	C	D	E	F	G	H	I	J	K	L	M
SBR-1502[a]	100	100	100	100	100	100	100	100	100	100	100	100	100
Zinc oxide	5	5	5	5	5	5	5	5	5	5	5	5	5
Stearic acid	2	2	2	2	2	2	2	2	2	2	2	2	2
Sulfur	2	2	2	2	2	2	2	2	2	2	2	2	2
CBS[b]	1	1	1	1	1	1	1	1	1	1	1	1	1
ZDC[b]	0.25	0.25	0.25	0.25	0.25	0.25	0.25	0.25	0.25	0.25	0.25	0.25	0.25
Mica[c]	—	10	20	30	40	10	20	30	40	10	20	30	40
A-187[d]	—	—	—	—	—	1	2	3	4	—	—	—	—
Si-69[e]	—	—	—	—	—	—	—	—	—	1	2	3	4

[a]Styrene-butadiene rubber, manufactured by Synthetics & Chemicals, Bareilly, India.
[b]N-cyclohexyl-2-benzthiazyl sulfenamide and zinc dithiocarbamate, manufactured by IEL Ltd., Rishra, India.
[c]3-micron muscovite mica, obtained from Mica Trading Corporation of India, Patna.
[d]Gamma glycidoxypropyltrimethoxy silane, obtained from Union Carbide U.K. Ltd., U.K.
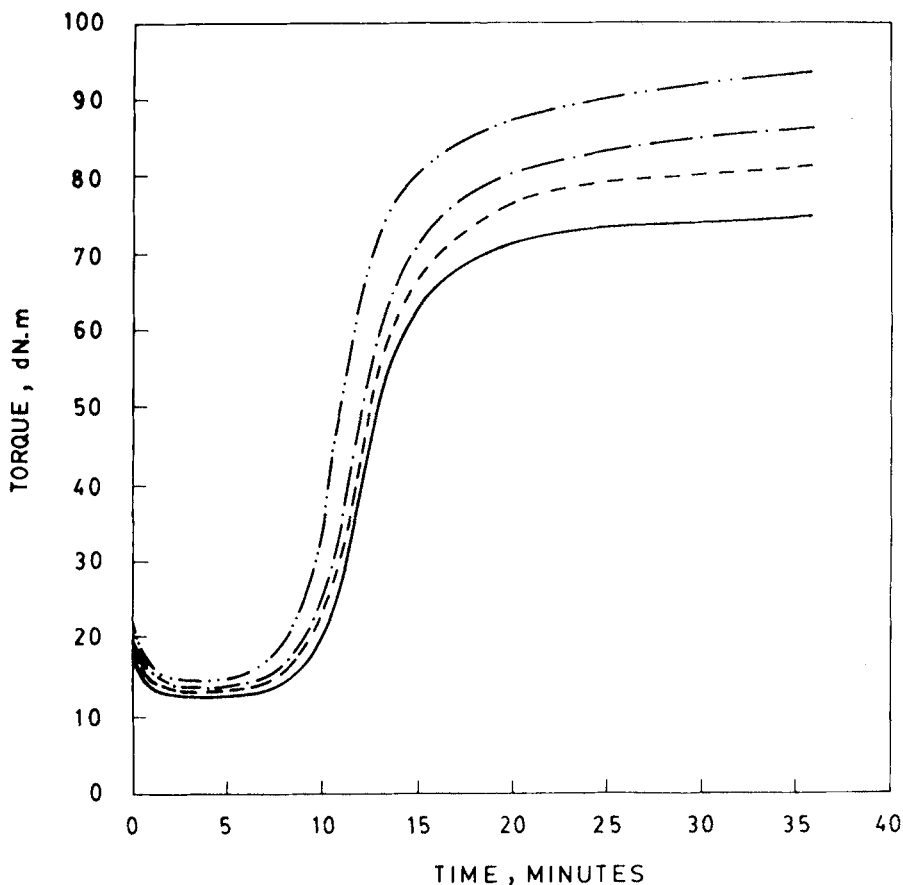[e]Bis-(3-triethoxy propyl)silyl-tetra sulfide, obtained from Degussa AG., F.R.G.

Fig. 1.   Rheographs of Si-69-treated mica-filled SBR mixes at 150°C: (-) 10 phr, (- - -) 20 phr, (-··-) 30 phr, and (-···-) 40 phr mica-filled stocks.

Scanning Electron Microscopy Studies

SEM observations of tensile, tear, and wear failure surfaces were made using a Philips 500 model scanning electron microscope. The failure surface of the test samples was carefully cut out and then sputter-coated with gold within 24 h of testing. The tilt was kept at 0° in all cases.

RESULTS AND DISCUSSION

Curing Characteristics

Representative rheographs and curing characteristics are shown in Figure 1 and Table II, respectively.

Cure rate decreases on addition of mica, indicating curative absorption on the filler surface. This is also manifested in optimum cure times. In case of A-187-treated mica, cure rate as well as optimum cure time remains nearly constant. Increase of optimum cure time, and consequently, decrease of cure

TABLE II
Processing Characteristics of the Mixes at 150°C Using Monsanto Rheometer (R-100)

							Mix no.						
	A	B	C	D	E	F	G	H	I	J	K	L	M
Minimum torque (dN.m)	10.5	11.2	12.0	12.8	13.6	12.5	13.0	13.0	13.5	12.5	13.5	14.0	14.5
Maximum torque (dN.m)	67.5	70.0	71.7	73.5	75.3	71.0	73.0	75.0	77.0	75.0	81.0	87.0	95.0
Optimum cure time (min)	15.5	17.0	17.5	17.5	17.5	15.0	15.0	15.0	15.0	18.0	18.0	19.0	20.0
Cure rate (min^{-1})	9.1	8.2	8.0	8.5	7.7	9.5	9.0	9.0	9.0	6.9	6.9	6.7	6.3
ML(1 + 4) at 120°C	29.0	30.0	32.0	33.0	33.0	29.0	30.0	32.0	33.0	30.0	32.0	34.0	35.0
Mooney scorch time at 120°C (min)	80.0	82.0	83.0	83.0	85.0	66.0	66.0	66.0	60.0	86.0	80.0	75.0	74.0

TABLE III
Physical Properties of Vulcanisates

	Mix no.												
	A	B	C	D	E	F	G	H	I	J	K	L	M
Tensile strength (MPa)	2.2	2.95	3.65	3.70	3.75	5.30	7.80	10.80	11.30	5.90	7.30	8.30	8.90
100% Modulus (MPa)	1.2	1.4	1.6	1.7	1.7	1.4	1.8	2.1	2.5	1.6	2.1	2.6	3.5
300% Modulus (MPa)	—	2.15	2.40	2.40	2.45	3.03	3.55	3.88	4.42	3.86	3.40	4.85	6.5
Elongation at break (%)	290	380	410	390	380	480	520	545	550	365	390	410	390
Tear Strength (kN/m)	12.4	13.7	15.1	21.1	19.9	22.8	25.5	28.8	29.2	17.0	25.0	27.7	28.8
Hardness (IRHD)	44.0	50.0	54.5	55.5	59.5	51.5	54.0	56.5	59.5	53.0	55.5	59.0	64.5
Density (g/cc)	0.98	1.08	1.12	1.16	1.20	1.08	1.12	1.15	1.21	1.08	1.13	1.16	1.21
Abrasion loss, (cc/h)	0.95	1.40	1.85	1.85	1.80	1.25	1.50	1.60	2.60	1.10	1.50	1.60	2.10
Resilience (%)	61.5	67.0	69.0	67.0	66.5	56.4	54.0	52.5	52.0	58.4	57.0	56.7	56.4
Heat build-up (°C)	9.0	10.0	10.0	13.0	14.0	13.0	16.0	20.0	23.0	15.0	19.0	22.0	26.0
Dynamic set (%)	0.6	2.1	0.9	1.1	1.2	2.0	2.0	2.0	2.2	0.8	0.8	0.7	0.6
Compression set at constant stress (%)	2.8	6.2	8.2	10.0	11.2	5.1	5.0	5.3	5.5	3.2	3.5	3.6	4.2
Compression set at constant strain (%)	14.6	24.3	28.7	42.0	41.7	19.5	21.0	22.4	19.5	14.2	15.0	15.5	14.0

rate in Si-69-treated stock has been attributed to the slow mica coupling agent reaction and slow crosslinking of SBR by Si-69.[8]

Maximum rheometric torque values increase on addition of the coupling agents. Improvement in modulus (Table III) is due to higher polymer-filler interaction. In case of Si-69, still higher torque (Fig. 1 and Table II), is due to the extra crosslinkings introduced through Si-69 itself.[8] Higher V_r values are an indirect indication of this type of crosslinking.

Silane coupling agents do not change the viscosity appreciably. The Mooney-scorch time at 120°C is very high. The decrease of scorch time on addition of silane coupling agents is due to secondary bond formation through coupling agents.[8]

Solvent Swelling of Rubber Vulcanisates

Figure 2 shows the change in V_r (apparent crosslink density) as a function of filler loading. In cases of untreated stock, decrease of V_r is due to adsorption of accelerators which has also been manifested by the higher elongation at break (Table III) at higher mica loading. The increase of V_r with the addition of A-187 and Si-69 coupling agents is due to higher polymer-filler interaction, as evident from Figures 3 to 5.
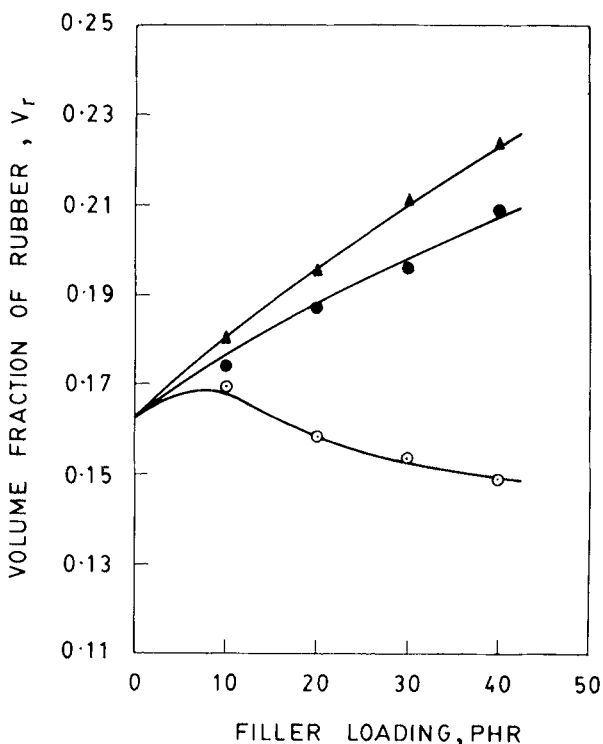

Fig. 2. Plots of volume fraction of swollen rubber as a function of filler loading: (○) mica-filled; (●) A-187-treated, and (▲) Si-69-treated mica-filled stocks.
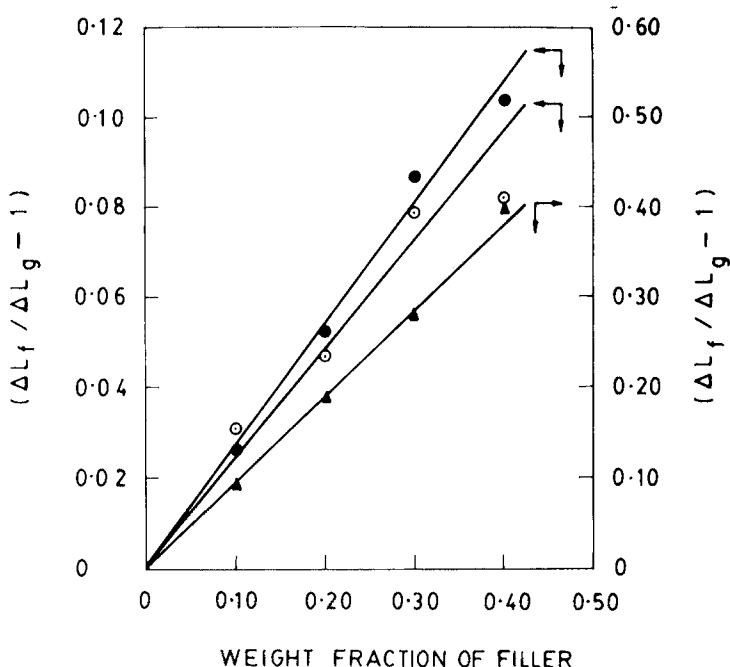
Fig. 3. Plots according to Westlinning-Wolff's equation [28]: (○) mica-filled; (●) A-187-treated, and (▲) Si-69-treated mica-filled stocks.

Mica-Rubber Interaction

Figure 3 shows the plots according to Westlinning–Wolff's equation (2)[28]

$$\alpha_F = \left(\frac{\Delta L_f}{\Delta L_g} = 1 \right) \Big/ w \qquad (2)$$

where, ΔL_f and ΔL_g are Rheometric torque differences between maximum and minimum torque values for filled and gum compounds, w is the weight fraction of filler to polymer. α_F, obtained from the slope of ($\Delta L_f/\Delta L_g = 1$) against w plot, is known to represent the filler activity. Figure 3 yields an α_F value 0.15 for untreated mica and 0.27 and 0.95 for A-187-treated and Si-69-treated mica, respectively. It is apparent that the higher values of ΔL_f are due to the enhanced polymer-filler interaction in presence of silane coupling agents.

Figure 4 shows the plots according to Cunnen-Russel equation (3)[29]

$$\frac{V_{ro}}{V_{rf}} = ae^{-z} + b \qquad (3)$$

where, V_{ro} and V_{rf} are the volume fraction of rubber in solvent-swollen gum and mica-filled vulcanisates, respectively. The ratio of V_{ro} to V_{rf} is a measure of polymer-filler interaction in filled system. z is the weight fraction of filler in polymer, a and b are two constants which depend on the filler activity. High
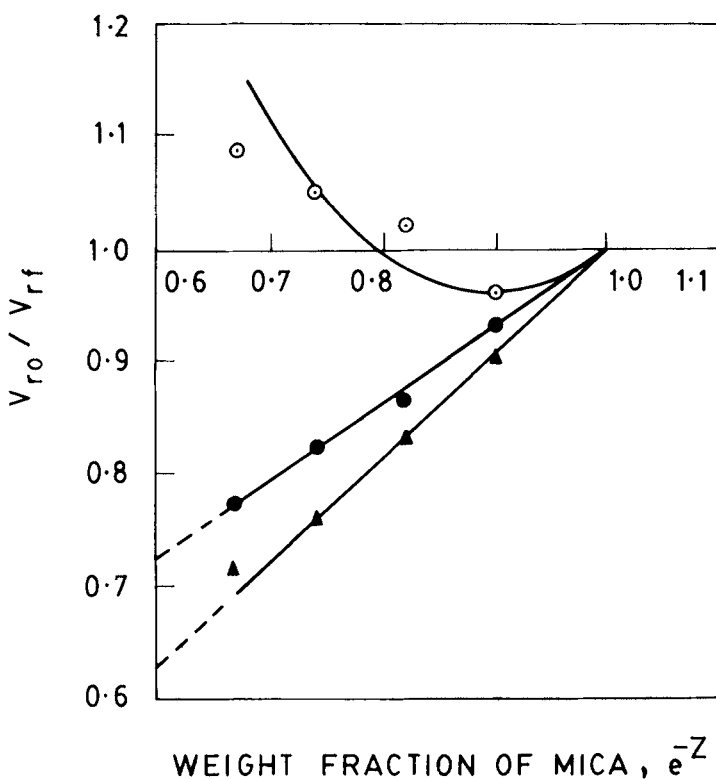
Fig. 4. Plots according to Cunnen-Russell equation [29]: (○) mica-filled, (●) A-187-treated, and (▲) Si-69-treated mica-filled stocks.

value of a and low value of b indicate strong polymer-filler attachment.[29] Untreated mica acts as a nonreinforcing filler, reflecting very poor rubber-filler interaction where $V_{ro}/V_{rf} > 1$.

But for A-187- and Si-69-treated mica composites, V_{ro}/V_{rf} values are always less than unity, which indicates higher polymer-filler interaction. It is also evident that the intercepts for untreated mica are higher than those of silane-treated stocks, indicating enhanced polymer-filler interaction due to the coupling agents.

Figure 5 shows the plot of V_{ro}/V_{rf} against $\theta/(1 - \theta)$ according to Kraus equations (4) and (5)[30]

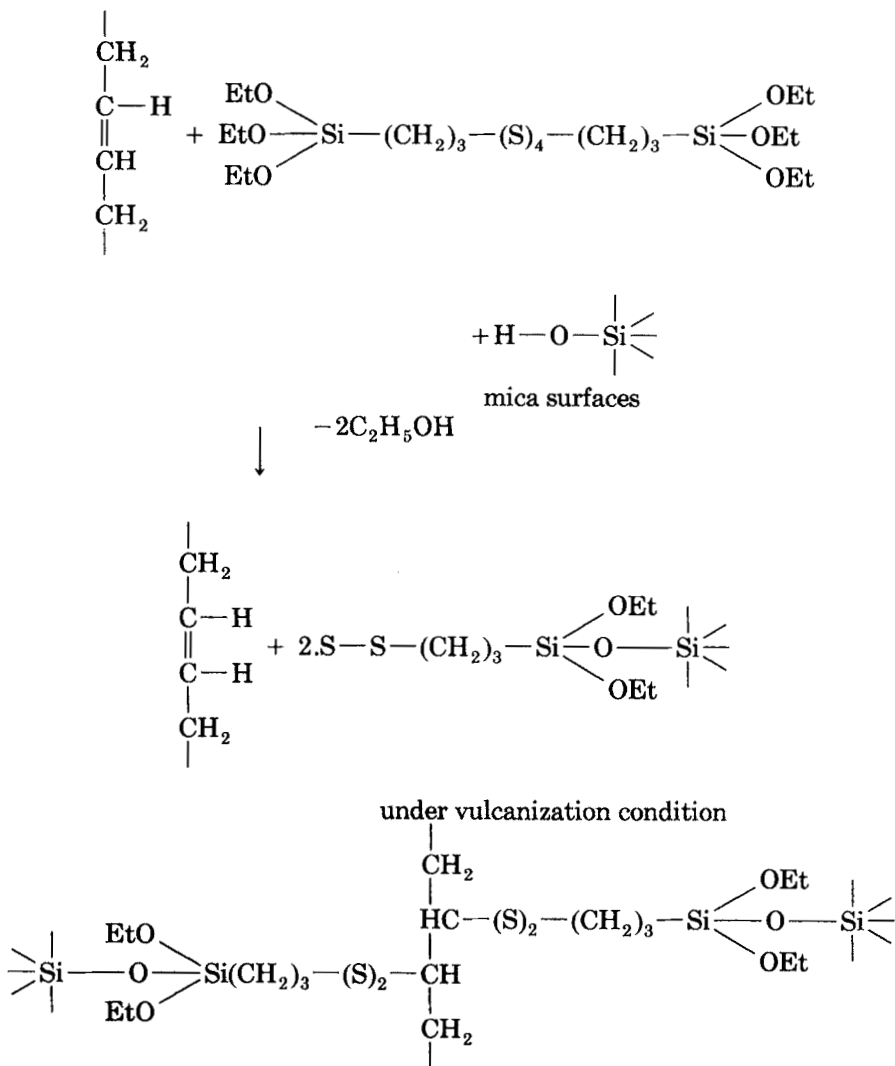$$\frac{V_{ro}}{V_{rf}} = 1 - \frac{m\theta}{(1 - \theta)} \tag{4}$$

where,

$$m = 3C\left(1 - V_{ro}^{1/3}\right) + V_{ro} - 1 \tag{5}$$

where, V_{ro} and V_{rf} are explained earlier, C is a constant characteristic of filler but independent of solvent. θ is the volume fraction of filler in the vulcanizate, m is designated as the 'polymer-filler interaction' parameter obtained

from the slope of the plot of V_{ro}/V_{rf} against $\theta/1 - \theta$. It is seen from Figure 5 that untreated mica shows a nonreinforcing trend beyond 3.0 volume percentage. However, both A-187- and Si-69-teated mica show reinforcing characteristics at all filler loadings studied due to enhanced polymer-filler interaction.

A mechanism of polymer-filler interaction due to the incorporation of Si-69 and A-187 in mica-filled SBR has been proposed.

$$\begin{array}{c} | \\ CH_2 \\ | \\ C-H \\ \| \\ CH \\ | \\ CH_2 \\ | \end{array} + \begin{array}{c} EtO \\ EtO-Si-(CH_2)_3-(S)_4-(CH_2)_3-Si \\ EtO \end{array} \begin{array}{c} OEt \\ OEt \\ OEt \end{array}$$

$$+H-O-Si\underset{|}{\overset{|}{<}}$$

mica surfaces

$$\downarrow \quad -2C_2H_5OH$$

$$\begin{array}{c} | \\ CH_2 \\ | \\ C-H \\ \| \\ C-H \\ | \\ CH_2 \\ | \end{array} + 2.S-S-(CH_2)_3-Si\underset{OEt}{\overset{OEt}{<}}O-Si\overset{|}{<}$$

under vulcanization condition

$$\begin{array}{c} | \\ CH_2 \\ | \\ HC--(S)_2-(CH_2)_3-Si\underset{OEt}{\overset{OEt}{<}}O-Si\overset{|}{<} \\ | \\ CH_2 \\ | \end{array}$$

$$\underset{EtO}{\overset{EtO}{>}}Si-O-Si(CH_2)_3-(S)_2-\begin{array}{c} | \\ CH_2 \\ | \\ CH \\ | \\ CH_2 \\ | \end{array}$$

The mechanism is self-explanatory. However, the salient features of the mechanism is that, one molecule of Si-69 couples through free radical mechanism with one olefinic unit of the elastomer molecule and also two molecules of —OH groups of mica, resulting in higher polymer-filler interaction. In case of A-187 ($CH_2\overset{O}{\frown}CH-CH_2-OC_3H_6-Si(OCH_3)_3$)-treated mica, the bridge between mica and coupling agent obviously forms through the elimination of one methyl alcohol. The other bridge between coupling agent and
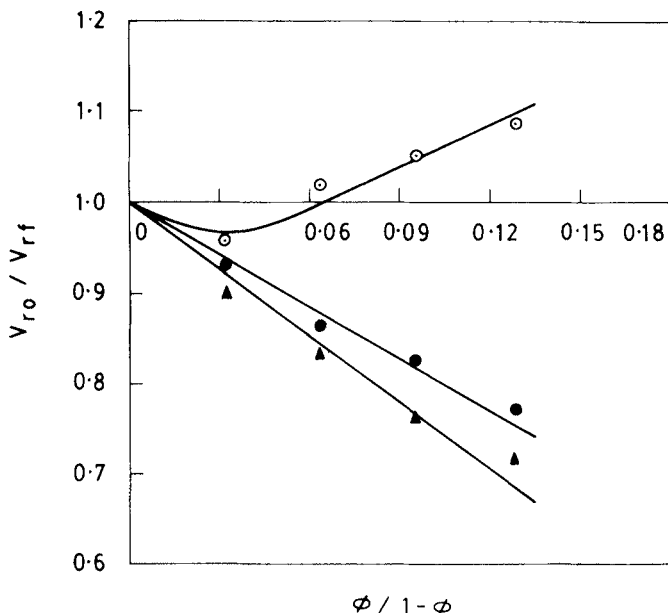
Fig. 5. Plots according to Kraus equation [30]: (○) mica-filled, (●) A-187-treated, and (▲) Si-69-treated mica-filled stocks.

polymer possibly involves interaction between active epoxy group of coupling agent with active tertiary hydrogen atom of butadiene monomer unit of SBR.

Physical Properties

Physical properties are summarized in Table III. Mica causes marginal increase in modulus and tensile strength. However, silane treatment causes noticeable improvement in these properties. This has been ascribed to en-hanced polymer-filler interaction.[7,8] Higher modulus and hardness of Si-69-treated mica composites over A-187-treated mica composites are obviously due to extra crosslinks through Si-69,[8] which imparts superior polymer-filler interaction to A-187-treated mica composites. Near constancy of elongation at break against mica loading for Si-69-treated stock in contrast to A-187-treated stock where EB% increases with filler loading reflects the enhanced polymer-filler interaction as well as formation of extra crosslink through Si-69. This is also manifested in the hysteresis values. Heat build-up (ΔT) increases in the presence of mica but the increase is more pronounced in the case of Si-69-treated filler than in A-187 ones. Similarly, resilience, dynamic set, and compression set at constant stress and at constant strain are lower in the case of silane-treated stock. However, the deterioration of abrasion resistance in silane-treated stock in contrast to reported results is not understood.

Stress-Strain Behavior

The stress-strain behavior of untreated and silane-treated mica-filled SBR vulcanisates is shown in Figure 6. Addition of mica does not make the vulcanisate rigid,[23] as is evident from higher percentage of elongation at break
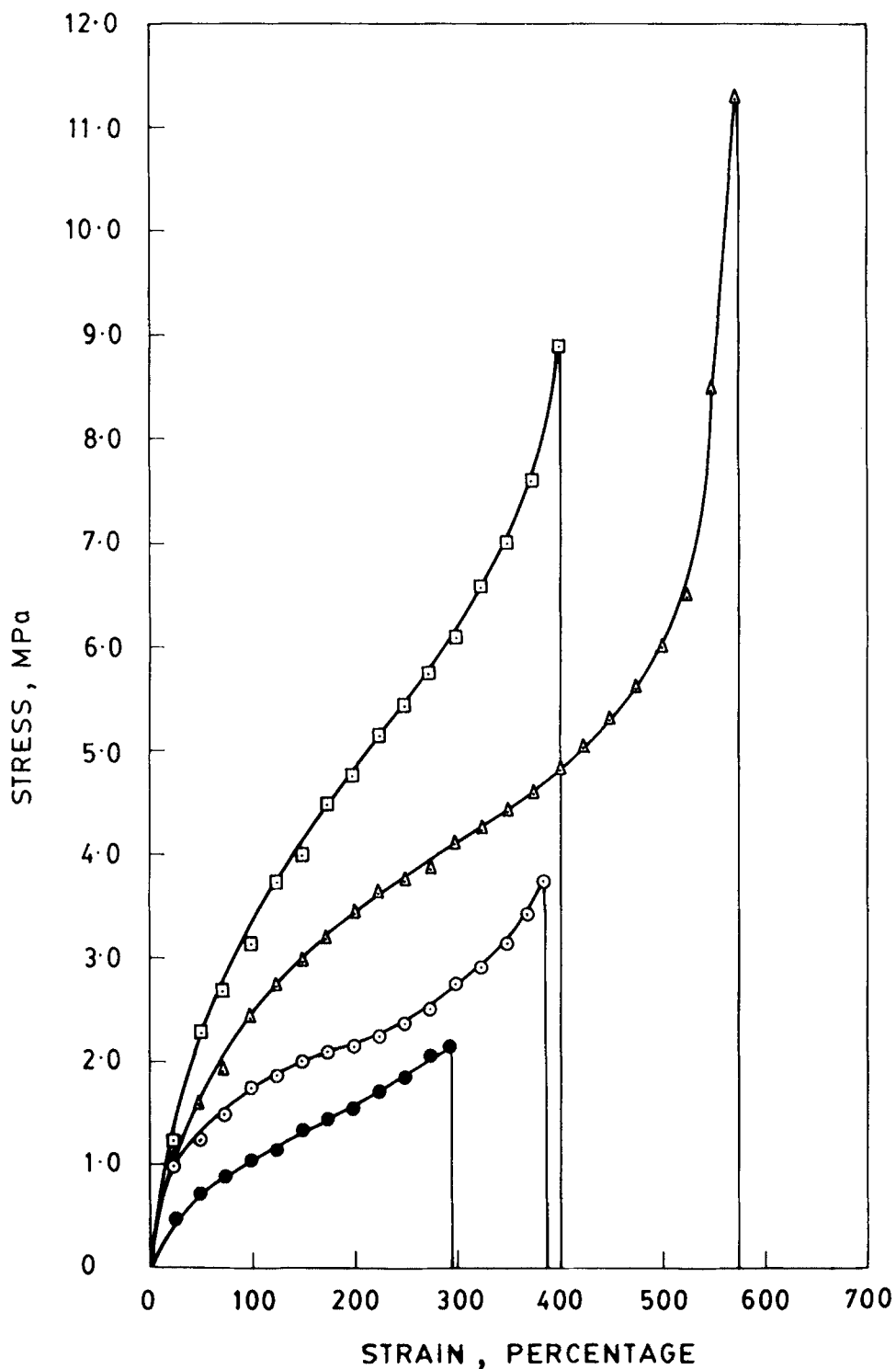
Fig. 6. Stress-strain curve of vulcanizates (●) gum; (○) 40 phr mica-filled, (△) 40 phr A-187-treated, and (□) Si-69-treated mica-filled vulcanizates.
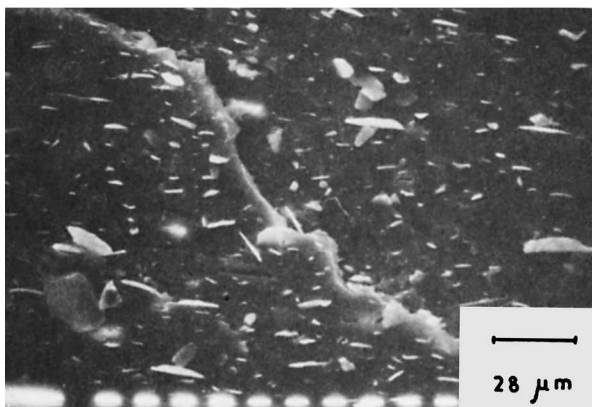
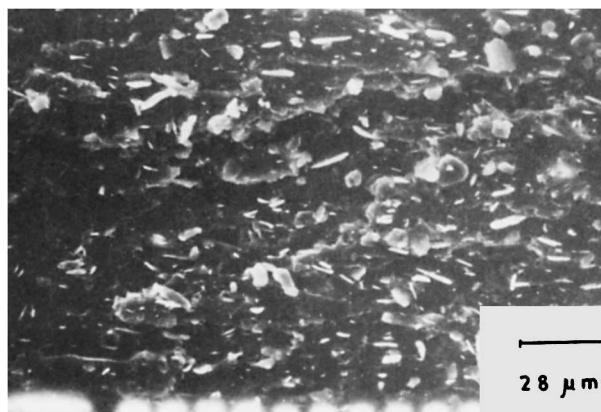Fig. 7.   Tensile fractograph of 30 phr mica-filled SBR composite (X400).

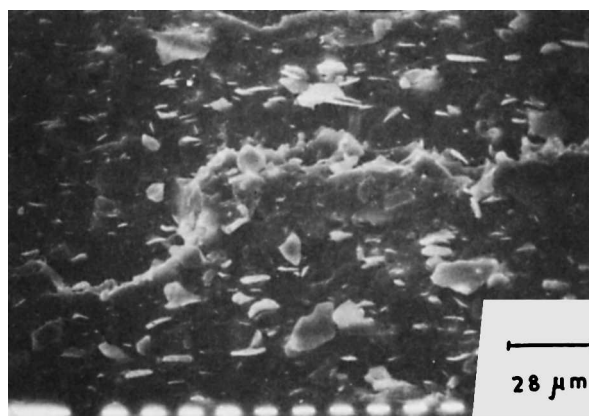Fig. 8.   Tensile fractograph of 20 phr mica-filled (Si-69 treated) SBR composite (X400).

Fig. 9.   Tear fractograph of 20 phr mica-filled SBR composite (X400).

at high mica loading. This is also manifested by significant flow region beyond initial Hookean rise of modulus. Silane-treated mica raises the modulus more than the untreated mica and initial slopes are also steeper particularly at higher mica loadings. Higher modulus of silane-treated mica is due to higher crosslink density than the untreated mica-filled vulcanisates. Higher modulus of Si-69-treated stock is due to the superior polymer-filler attachment and extra crosslinks through Si-69, which itself acts as a curing agent[8] by virtue of its tetrasulfide functionality. The sharp rise of stress in case of 30 and 40 phr mica-loaded vulcanizates, particularly in silane-treated stock, is an indirect proof of enhanced polymer-filler attachment and orientation of mica[23] which is also evident from SEM fractographs (see Figs. 8 and 10) discussed later in this article.

Scanning Electron Microscopy

Figure 7 shows the tensile fractograph of mica-filled composites where straight fracture path and debonded mica particles indicate poor polymer-filler
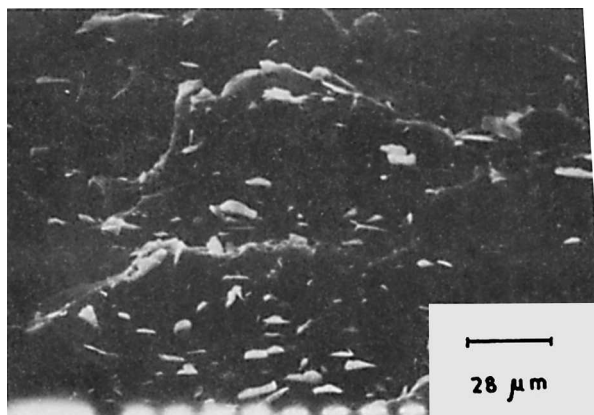

Fig. 10.   Tear fractograph of 20 phr mica-filled (Si-69 treated) SBR composite (X400).
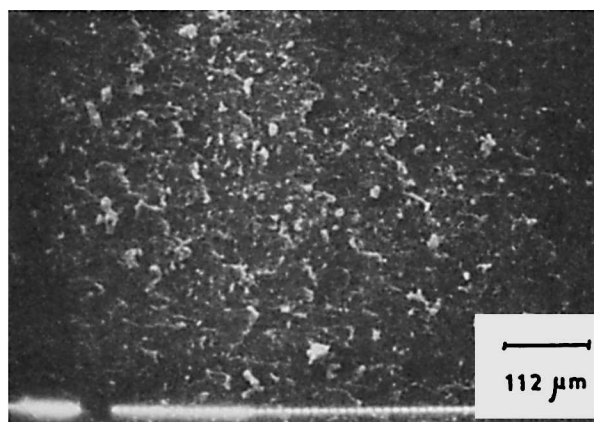

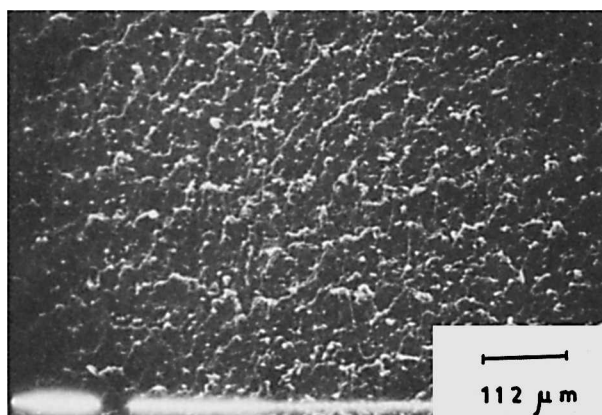Fig. 11.   Wear fractograph of 20 phr mica-filled SBR composite (X100).

Fig. 12. Wear fractograph of 20 phr mica-filled (Si-69 treated) SBR composite (X100).

interaction, whereas in Si-69-treated stock (Fig. 8), rough failure surface and increased wetting of mica by the matrix shows higher polymer-filler interaction.

Tear fractographs behave similarly. Rough tear surface of Si-69-treated mica-filled stock (see Fig. 10) over smooth fracture surface of untreated mica-filled stock (Fig. 9) again shows superior polymer-filler interaction with Si-69. Oriented mica particles are also observed in case of Si-69-treated stocks (Figs. 8 and 10).

Fractograph of wear surface of mica-filled composite (Fig. 11) show deformed ridges as well as lumpy materials, showing poor abrasion resistance, but Si-69-treated stock (Fig. 12) shows deformed ridges and dimple formation indicating higher fatigue life. However, abrasion loss values (Table III) could not be correlated with the fractograph. It is also found from Figures 7 and 8 that addition of Si-69 influences the orientation of mica particles and is responsible for higher strength at higher elongation in A-187- and Si-69-treated stocks over simple mica-filled stock (Fig. 6). Fractographs of A-187-containing composites are similar to Si-69-containing composites.

CONCLUSION

Mica marginally improves the tensile properties of styrene-butadiene rubber, but abrasion loss and set properties deteriorate. Incorporation of silane coupling agent enhances mica-rubber interaction, which in turn is responsible for increase in tensile, modulus, set, and hysteresis properties. Marginally, higher viscosity of silane-treated stocks reflect secondary structure formation in presence of silane coupling agent. Scanning electron microscopic (SEM) photomicrographs also show enhanced polymer-filler interaction in the presence of silanes. Oriented mica particles are also found in SEM fractographs, which might be responsible for the increase in the stress at higher elongation, particularly in cases of higher mica loading.

References

1. R. T. Woodhams and M. Xanthos, *Handbook of Fillers and Reinforcements of Plastics*, J. V. Milewski and H. S. Katz, eds., Van Nostrand Reinhold, New York, 1978, p. 344.

2. S. R. Locke, R. Lindsay, and M. Fenton, "The properties of suzorite mica flake as a reinforcement in plastics composites," 30th Annual Technical Conference, Reinforced Plastics/Composites Institute, The Society of the Plastics Industry, Section 4-D (1975).

3. B. Fisa, B. Sanchagrin, and B. D. Favis, *Polym. Compos.*, **5**(4), 264 (1984).

4. M. Xanthos, G. C. Hawley, and J. Antonacci, 34th Annual Technical Conf. SPE Preprints, 582 (1976).

5. A. Garton, *Polym. Compos.*, **3**(4), 189 (1982).

6. Mitsubishi Petrochemical Co., Japanese Patent 760, 41 (1981).

7. Union Carbide Corporation, "Organic Functional Silane-A Profile," Technical Brochure (1981).

8. F. K. Lautenschlaeger and K. Edwards, Model Compound Vulcanisation, Part V, p. 16, ACS Meeting, 1979, Atlanta, GA.

9. S. J. Monte and G. Sugerman, "Ken React reference manual," Kenrich Petrochemicals Inc., Bulletin No. KR-1084L-1 (1985).

10. S. F. Tausz and C. E. Chaffey, *J. Appl. Polym. Sci.*, **27**, 4493 (1982).

11. T. Vu-Khanh, B. Sanchagrin, and B. Fisa, *Polym. Compos.*, **6**(4), 249 (1985).

12. T. Vu-Khanh, B. Sanchagrin, and B. Fisa, Composites 85 Symposium, NRCC/IMRI, Boucherville, Quebec, Canada, pp. 9.1–9.47, Nov. 20 (1984).

13. T. Vu-Khanh and B. Fisa, *Polym. Compos.*, **7**(4), 219 (1986).

14. S. F. Xavier and Y. N. Sharma, *Polym. Compos.*, **7**(1), 42 (1986).

15. H. P. Schreiber, Y. B. Tewari, and M. R. Wertheimer, *J. Appl. Polym. Sci.*, **20**, 2663 (1976).

16. B. Fisa and L. A. Utracki, *Polym. Compos.*, **5**(1), 36 (1984).

17. K. Okuno and R. T. Woodhams, *J. Polym. Eng. Sci.*, **15**(4), 308 (1975).

18. L. A. Utracki, *Polym. Compos.*, **7**(5), 274 (1986).

19. M. R. Wertheimer, L. Paquin, H. P. Schreiber, and S. A. Boggs, *IEEE Trans. on Elec. Insul.*, **EI-12**, April 2 (1972).

20. M. R. Wertheimer, L. Paquin, and H. P. Schreiber, *J. Appl. Polym. Sci.*, **20**, 2665 (1976).

21. R. J. Eldred, *Rubber World*, **188**(6), 26 (1983).

22. J. A. William, U.S. Natl. Tech. Inform. Service, AD Rep., 750, 595 (1972).

23. S. Debnath, S. K. De, and D. Khastgir, *J. Math. Sci.*, in press.

24. S. Debnath, A. K. Bhattacharya, D. Khastgir, and S. K. De, *Kautschuk Gummi Kunststoffe*, **40**, 938 (1987).

25. S. Debnath, P. P. De and D. Khastgir, *Rubber Chem. Technol.*, in press.

26. S. Debnath and D. Khastgir, *J. Elastomers and Plast.*, in press.

27. B. Ellis and G. N. Welding, *Techniques of Polymer Science*, Soc. Chem. Ind., London, 1964, p. 46.

28. H. Westlinning and S. Wolff, *Kautsch. Gummi Kunstst.*, **19**, 470 (1966).

29. J. I. Cunnen and R. M. Russell, *J. Rubber Res. Inst. Malaya*, **22**, 308 (1969); *Rubber Chem. Technol.*, **43**, 1215 (1970).

30. G. Kraus, *J. Appl. Polym. Sci.*, **7**, 861 (1963).